Human Opioid Peptide Met-Enkephalin Binds to Anionic Phosphatidylserine in High Preference to Zwitterionic Phosphatidylcholine: Natural-Abundance ^{13}C NMR Study on the Binding State in Large Unilamellar Vesicles†

Tomohiro Kimura*

Institute for Chemical Research, Kyoto University, Uji, Kyoto 611-0011, Japan

Received August 12, 2006; Revised Manuscript Received October 12, 2006

ABSTRACT: A human opioid neuropeptide, Met-enkephalin (M-Enk: Tyr[1]-Gly[2]-Gly[3]-Phe[4]-Met[5]), having no net charge binds to anionic phosphatidylserine (PS) in high preference to zwitterionic phosphatidylcholine (PC). The binding mechanism in the PS and PC bilayers was studied on the basis of the inter- and intramolecular interaction data obtained by natural-abundance ^{13}C nuclear magnetic resonance (NMR) of the peptide. Prominent upfield changes of the ^{13}C resonance were observed in the C-terminal residue upon binding to PS, whereas no such marked change was observed upon binding to PC. The upfield chemical shift changes with their characteristic carbon site dependence are ascribed to the electrostatic binding between the peptide C-terminal CO_2^- and the PS headgroup NH_3^+. Despite the net negative charge of the PS bilayer surface, M-Enk thus anchors the negatively charged C-terminus. In the N-terminal residue, on the other hand, marked downfield chemical shift changes are observed upon binding to both the PS and PC bilayers, the magnitude of the changes being much larger in the PS system. The downfield changes with their characteristic carbon site dependence are ascribed to the electrostatic binding between the peptide N-terminal NH_3^+ and the lipid headgroup negative charge(s) (CO_2^- or PO_4^- in PS, PO_4^- in PC). Perturbation on the signal half-widths due to membrane binding also indicates the preferential and deeper binding of M-Enk on the PS membrane surface than on the PC membrane surface. Local charge cancellation takes place efficiently between M-Enk termini and the PS headgroups and compensates for the strong electrostatic hydration of the ionic groups. Distribution of the charged (positive and negative) and uncharged sites in the headgroups along the bilayer normal is responsible for the marked difference between PS and PC headgroups in controlling the binding state of the zwitterionic M-Enk.

Many of physiologically vital peptides bind from bulk water to phospholipid membrane surface, in order to function through harmonious and opposing contributions of various types of interactions, such as electrostatic and hydrophobic, at atomic resolution (*1*, *2*). With respect to neuropeptides, knowledge on such detailed peptide−lipid interactions (*3*) is essential to establish fundamental biochemistry on delicate physiological roles of phospholipids in regulating equilibrium and kinetics of the neuropeptide−receptor binding (*4*, *5*). In this work, the binding state of a human opioid peptide, Met-enkephalin, Tyr[1]-Gly[2]-Gly[3]-Phe[4]-Met[5] (M-Enk) (*6*), in two different model membranes composed of phosphatidylcholine (PC)[1] or phosphatidylserine (PS) is investigated by means of natural-abundance ^{13}C nuclear magnetic resonance (NMR) spectroscopy. According to the ^{13}C NMR data on peptide−lipid interactions, the mechanism of a notable binding phenomenon is discussed: membrane binding of M-Enk with no net charge is largely enhanced by increasing content of the anionic PS in zwitterionic PC membranes (*7*, *8*). While the conformation of enkephalin in various types of phospholipid membranes is being elucidated as the peptide internal structure (*8*−*13*), how the location and orientation of the peptide are controlled on the membrane surface remains unsolved.

Microscopic probing of the peptide−lipid binding interactions on the membrane surface is important in revealing the mechanism of binding, which is expected to depend on the lipid headgroup species. ^{13}C NMR spectroscopy can provide valuable information on the binding interactions such as through the chemical shifts (δ) and broadening (T_2) of the peptide signals. The usefulness of this method largely relies on its high atomic site distinguishability and sensitivity to the molecular environment. Previously, I studied in collaboration the binding mechanism of a neuropeptide achatin-I (Gly[1]-D-Phe[2]-Ala[3]-Asp[4]) in egg yolk PC membrane by means of ^{13}C NMR in combination with fine-structure analysis of the ^1H NMR (*3*). It was unveiled that the binding of achatin-I to the zwitterionic PC takes place both by the N-terminal α-NH_3^+ and by the C-terminal Asp[4] α- and β-CO_2^-, with shallow anchoring of the hydrophobic side chain of the D-Phe[2] residue. The binding site of the negatively charged

† This work was made possible by the 21st Century Center of Excellence Program in Japan.

* Corresponding author. Present address: Laboratory of Membrane Biochemistry and Biophysics, NIAAA, National Institutes of Health, Bethesda, MD 20892. Phone: (301) 435-6727. Fax: (301) 594-0035. E-mail: kimurato@mail.nih.gov.

[1] Abbreviations: M-Enk, Met-enkephalin; PC, phosphatidylcholine; PS, phosphatidylserine; NMR, nuclear magnetic resonance; FID, free induction decay; LUV, large unilamellar vesicles; SUV, small unilamellar vesicles; egg yolk PC, egg yolk phosphatidylcholine; POPS, 1-palmitoyl-2-oleoyl-*sn*-glycero-3-phospho-L-serine; lysoPC, 1-palmitoyl-*sn*-glycero-3-phosphocholine; lysoPS, 1-palmitoyl-*sn*-glycero-3-phospho-L-serine.

10.1021/bi061641v CCC: $33.50
Published on Web 12/01/2006

C-terminal Asp[4] is the headgroup $N(CH_3)_3^+$ in the most superficial region of the PC membrane, nevertheless, at the substantial expense of the strong electrostatic hydration of the CO_2^- groups. The ^{13}C NMR method is suitable to clarify differences between the anionic PS and the zwitterionic PC membranes in the site-specific binding interactions with M-Enk.

Does the N-terminal NH_3^+ of M-Enk bind to the negatively charged site CO_2^- or PO_4^- in the anionic PS headgroup, as can be intuitively expected from the effect of the net minus charge of PS at neutral pH (*7*, *8*, *14*−*17*)? Does the N-terminal NH_3^+ bind to the negatively charged site PO_4^-, on the other hand, in the zwitterionic PC with no net charge? Regarding the electrostatic binding of the C-terminal CO_2^-, it is of particular interest to elucidate whether the binding with the NH_3^+ in the PS headgroup takes place or not; recall the result from the molecular dynamics simulation on the PS (dipalmitoylphosphatidylserine) membrane which showed that the NH_3^+ possessing a charge sign opposite to the net charge of the headgroup is buried under the negatively charged groups CO_2^- and PO_4^- (*18*).

When we analyze the binding interactions according to ^{13}C NMR data, it should be noted that the perturbation on the ^{13}C signals of the peptide upon membrane binding reflects in general both the intermolecular (interactions with lipid and water molecules) and intramolecular (conformational) effects. However, we can look into the inter- and intramolecular effects by varying the extent of the intermolecular effects on the ^{13}C resonance by, for example, varying the surface curvature of the membrane system. This analytical scheme is accessible according to the previous findings on the enkephalin conformation on the membrane surface; enkephalin folds the short backbone irrespective of the type of PC and PS membranes [micelles, bicelles, small unilamellar vesicles (SUV), or large unilamellar vesicles (LUV)] in a common way of separating the hydrophilic and hydrophobic moieties in the peptide structure (*8*−*12*), while it takes a random coil conformation in bulk water (*10*, *19*, *20*). In this work, the binding state of the folded M-Enk on the membrane surface is discussed on the basis of the binding-interaction data extracted in the ^{13}C NMR.

Large unilamellar vesicles, LUV, are one of the widely adopted models for biological membranes to conduct physicochemical studies, especially because of the absence of surface-curvature effects (*3*, *21*, *22*). In studying the binding mechanism of a peptide on the membrane surface, it is considered to be important to use such a membrane system with a negligible curvature, as the peptide−lipid interactions near the water−membrane interface are likely to be sensitive both to the degree of lipid packing and to the accompanying change in the degree of hydration. Indeed, it is known that the curvature effect is substantial on the dynamics of smaller lipid assemblies such as the SUV (diameter of ∼50 nm) and micelles (diameter of ∼5 nm). In general, the large structural fluctuations and extensive hydration to the acyl chains due to the curved surface have been utilized in probing signals of transmembrane peptides and proteins in solution-state NMR (*1*, *23*). As for superficially binding peptides, in contrast, a more careful account of the hydration effect is necessary, as the binding is always accompanied by release of water molecules from hydrated peptide (*3*, *24*, *25*) and lipids (*26*−*28*). Here, a systematic comparison among the LUV, SUV, and micelles is made on the binding interactions with M-Enk.

EXPERIMENTAL PROCEDURES

Materials. Met-enkephalin (M-Enk: Tyr[1]-Gly[2]-Gly[3]-Phe[4]-Met[5]) was obtained from the Peptide Institute (Minoh, Japan). Egg yolk phosphatidylcholine (egg yolk PC) and 1-palmitoyl-2-oleoyl-*sn*-glycero-3-phospho-L-serine (POPS) used to prepare vesicles were from NOF (Tokyo, Japan) and Avanti (Alabaster, AL), respectively. Egg yolk PC was used for PC as in the previous study on the membrane binding of a neuropeptide achatin-I (*3*). The PC and PS membranes are in the liquid-crystalline state at the investigated temperature of 30.0 ± 0.1 °C; the transition temperature between the gel and liquid-crystalline phases is at −15 to −7 °C for egg yolk PC (*29*) and at 14 °C for POPS (*30*). 1-Palmitoyl-*sn*-glycero-3-phosphocholine (lysoPC) and 1-palmitoyl-*sn*-glycero-3-phospho-L-serine (lysoPS) used for the preparation of micelles were from Sigma (St. Louis, MO). The anionic POPS and lysoPS were monosodium salts, and the zwitterionic egg yolk PC, lysoPC, and M-Enk were in the free form, to avoid deionization of the peptide and lipids due to the acidification or basification of the samples when dissolved in water. Solvent heavy water (D_2O: 99.90% D) was from Euriso-top (Saint Aubin, France).

The mixture of M-Enk and the PC membrane (PC−LUV, −SUV, or −micelles) in D_2O was prepared at concentrations of 2 and 20 mM for the peptide and lipid, respectively. The mixture of M-Enk and the PS membrane (PS−LUV, −SUV, or −micelles) in D_2O was at 5 and 50 mM for the peptide and lipid, respectively. Stronger binding of M-Enk to PS than to PC results in much broader ^{13}C NMR signals of M-Enk on the PS system. Thus the concentrations are increased for the PS system at the fixed lipid/peptide molar ratio to determine the chemical shift values with a low noise level. Here a difference in the binding equilibrium due to the concentration modification within the same order of magnitude was approximately neglected, and differences in the binding state between the PC and the PS membranes are discussed. At the concentrations examined, the effect of intermolecular peptide−peptide interactions on the binding state is negligible due to the large molar ratio of the lipid to the bound peptide on the order of 10^2−10^3. The LUV were prepared by the extrusion method, and the SUV were prepared by the sonication method as described elsewhere (*3*, *31*). The diameters of the vesicles and micelles prepared were ∼100 nm for the LUV, ∼50 nm for the SUV, and ∼5 nm for the micelles. The mixture of the peptide and membrane (LUV, SUV, or micelles) was made by dissolving the solid peptide in the membrane dispersion. As a reference state in examining the binding from bulk water, M-Enk in D_2O was prepared at the concentration of 2 mM.

^{13}C NMR Measurements. Natural-abundance ^{13}C NMR was measured for (1) the mixture of M-Enk and the membrane and (2) M-Enk in aqueous solution on a JEOL (Tokyo, Japan) 600 MHz spectrometer (JNM-ECA600 model with a superconducting magnet of 14.10 T) operating at the ^{13}C frequency of 151 MHz. The spectrometer was equipped with a probe for the sample tube of 10 mm o.d. The data points of 32768 were sampled over the spectral range of 250 ppm for the digital resolution of 0.0076 ppm (1.2 Hz). 25000−

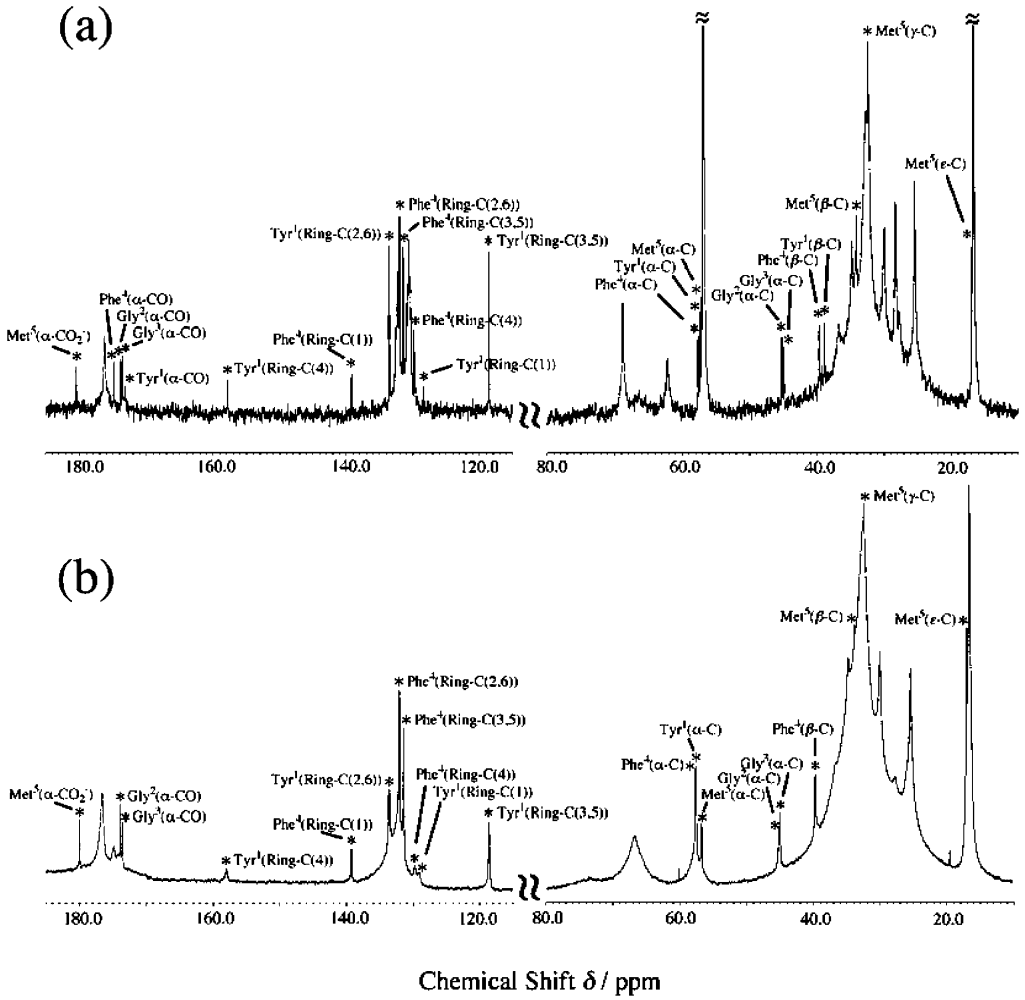

FIGURE 1: Natural-abundance ^{13}C NMR spectra of (a) M-Enk (2 mM) and PC (20 mM)−LUV and (b) M-Enk (5 mM) and PS (50 mM)−LUV recorded on a JNM-ECA 600 MHz spectrometer (JEOL) operating at a ^{13}C frequency of 151 MHz. Signals with an asterisk are from M-Enk assigned as shown. 85000−230000 scane of free induction decay (FID) signals were acquired for the PC and PS systems, respectively, with a probe for a 10 mm o.d. sample tube. 230000 scans for the PS system, corresponding to a 7 day accumulation, were carried out to gain signal-to-noise ratios large enough to determine chemical shifts of the broad peptide signals within the uncertainty of the digital frequency resolution. FID signals were processed with the exponential apodization function at the broadening factor of 5.0 Hz.

230000 scans of free induction decay (FID) signals were acquired. The maximum number of scans (230000) corresponding to a 7 day accumulation was for the mixture of M-Enk and the PS−LUV. The strong binding of M-Enk to the surface of the PS−LUV with no significant curvature requires the long accumulation to determine the peptide chemical shifts at high signal-to-noise ratios. The PS vesicles were confirmed by ^{1}H NMR analysis to be stable for the duration of the measurement. The ^{13}C chemical shifts (δ) relative to the DSS (sodium 2,2-dimethyl-2-silapentane-5-sulfonate) methyl carbons were obtained by referring to the absorption frequency of the solvent deuteron monitored as the lock signal. The assignment of ^{13}C signals of M-Enk was made according to the previous report (*32*).

Ultracentrifugation Experiments. The fraction of bound M-Enk to the LUV was estimated by the ultracentrifugation experiment as described elsewhere (*3*). The method enables us to separate the membrane-bound peptides in the top fraction as pellets from the free peptides dissolving in the bottom fraction of D_2O. The experiment was carried out on a Beckman (Fullerton, CA) TL-100 instrument equipped with a rotor TLA-100.2 model. Centrifuging conditions were 230000*g* at 30 °C for 2 h for the PC−LUV and 320000*g* at 30 °C for 4 h for the PS−LUV.

RESULTS AND DISCUSSION

Distinctions between the zwitterionic PC and the anionic PS membranes in microscopic site−site binding interactions with the zwitterionic M-Enk are investigated by means of the natural-abundance ^{13}C NMR spectroscopy. Well-resolved NMR from all of the carbon sites in the peptide structure makes it possible to gain a schematic insight into the membrane-binding phenomenon.

PS Binding in High Preference to PC Binding. The spectra observed for the mixtures of M-Enk (a) with the PC−LUV and (b) with the PS−LUV are shown in Figure 1. M-Enk gives the ^{13}C signals (marked by an asterisk with the assignment) as an average for membrane-bound and free states due to rapid exchange in the NMR time scale. The membrane-binding effects on the half-widths and on the chemical shifts of the peptide signals are more drastic in the PS system than in the PC system. The measured changes in the half-widths and chemical shifts upon membrane binding are carbon site dependent. Details are discussed below.

Table 1: Observed ^{13}C Chemical Shifts δ (ppm) of Met-Enkephalin in Bulk Water, in the Mixture with PC−LUV, and in the Mixture with PS−LUV[a]

			PC		PS	
amino acid residue	carbon site	in bulk water (obsd)	in mixture with PC−LUV (obsd)	$\Delta\delta$ induced by membrane binding	in mixture with PS−LUV (obsd)	$\Delta\delta$ induced by membrane binding
Tyr[1]	α-C	57.35	57.37	+0.02	57.56	+0.21
	α-CO	172.96	173.14	+0.18	−[b]	–
	β-C	38.77	38.85	+0.08	−[b]	–
	ring-C(1)	128.32	128.36	+0.04	129.07	+0.75
	ring-C(2,6)	133.54	133.52	−0.02	133.51	−0.03
	ring-C(3,5)	118.59	118.58	−0.01	118.54	−0.05
	ring-C(4)	157.89	157.90	+0.01	158.03	+0.14
Gly[2]	α-C	45.20	45.20	0.00	45.23	+0.03
	α-CO	173.83	173.82	−0.01	173.88	+0.05
Gly[3]	α-C	44.90	44.91	+0.01	45.06	+0.16
	α-CO	173.50	173.50	0.00	173.53	+0.03
Phe[4]	α-C	57.61	57.62	+0.01	57.74	+0.13
	α-CO	174.81	174.78	−0.03	−[b,c]	–
	β-C	39.63	39.63	0.00	39.70	+0.07
	ring-C(1)	139.21	139.22	+0.01	139.22	+0.01
	ring-C(2,6)	131.95	131.95	0.00	132.03	+0.08
	ring-C(3,5)	131.44	131.43	−0.01	131.38	−0.06
	ring-C(4)	129.84	129.82	−0.02	129.69	−0.15
Met[5]	α-C	57.15	57.13	−0.02	56.80	−0.35
	α-CO_2^-	180.42	180.39	−0.03	179.93	−0.49
	β-C	33.98	33.99	+0.01	33.81	−0.17
	γ-C	32.23	32.24	+0.01	32.37	+0.14
	ϵ-C	16.84	16.85	+0.01	16.95	+0.11

[a] The chemical shift change $\Delta\delta$ (ppm) due to the binding from bulk water to the membrane surface has been measured for all of the carbon sites. Free induction decay (FID) signals were accumulated until it was confirmed that the signal-to-noise ratios were gained enough to analyze the chemical shifts δ within the uncertainty due to digital frequency resolution on the order of mppm. Met-enkephalin (M-Enk: Tyr[1]-Gly[2]-Gly[3]-Phe[4]-Met[5]) and the PC membrane (PC−LUV, −SUV, or −micelles) in D_2O were prepared at the concentrations of 2 and 20 mM for the peptide and lipid, respectively. M-Enk and the PS membrane (PS−LUV, −SUV, or −micelles) in D_2O were prepared at 5 and 50 mM for the peptide and lipid, respectively. M-Enk in D_2O was prepared at 2 mM. [b] Value not determined because of a signal broadening. [c] Value not determined because of an overlap with the lipid signal.

Signal Broadening Due to Membrane Binding. Signal broadening in response to the transfer from bulk water to the membrane surface provides information on molecular dynamics of the membrane-binding phenomenon; note that the NMR line broadening depends in general both on the site-specific slowdown of motion at atomic sites observed and on the overall rate of exchange between the membrane-bound state and the free state in bulk water. Here, by examining the carbon site dependence of the signal broadening, an attempt is made to look into the carbon site dependent slowdown of molecular motion. Among the carbons in M-Enk, signals at the α-CO and β-C sites which are within or close to the backbone in the N-terminal Tyr[1] were not detected in the mixture with PS−LUV. This extreme case of line broadening indicates marked slowdown of motion at the peptide N-terminus due to strong interaction with the PS membrane.

As seen in the spectrum region of ∼120−160 ppm in Figure 1b, substantial broadening of M-Enk signals takes place at the aromatic carbons in the Tyr[1] and Phe[4] residues upon binding to PS in the LUV. As much as +44 Hz was observed at the ring-C(4) in Phe[4], +35 Hz at the ring-C(1) in Tyr[1], and +33 Hz at the ring-C(4) in Tyr[1]. Notable broadening at the aromatic ring carbons in the Tyr[1] and Phe[4] side chains indicates anchoring of these hydrophobic rings on the surface of the PS membrane. The anchoring was confirmed in the corresponding ^1H NMR spectrum; the ring-H signals with the fine structures merge due to broadening and shift upfield upon binding to the PS membrane (see Figure S1 in Supporting Information). In contrast to the PS-binding in the LUV, broadening was not significant in the case of PC-binding in the LUV; the largest increase in the ^{13}C signal half-width is only +4 Hz at the ring-C(1) in the N-terminal Tyr[1] residue. According to the above results, it is evident that binding of M-Enk having no net charge is stronger at the anionic PS than at the zwitterionic PC. In previous reports, it was shown that the binding of enkephalin was enhanced by increasing the content of PS in the PC membrane, a result from the ^{13}C spin−lattice relaxation time (T_1) of the α-carbon enriched in the Gly[2] or Gly[3] residue (*7*) and a result from the transferred nuclear Overhauser effect (TrNOE) in ^1H NMR monitoring the peptide conformational change in response to the membrane binding (*8*). The conclusion here of the stronger binding to PS than to PC is further supported by the ultracentrifugation experiment. The fractions of the bound M-Enk, which is in rapid exchange with the free state in bulk water as observed by the peptide ^{13}C NMR, was estimated to be ∼15% on the PS−LUV and less than a few percent on the PC−LUV.

Chemical Shift Changes. Next let us examine the site−site binding interactions between M-Enk and phospholipids on the membrane surface, based on the static information provided by the ^{13}C chemical shifts. Since the conformation of enkephalin on the membrane surface is common to the PC and the PS membranes, i.e., with a folded backbone to segregate the hydrophilic and hydrophobic moieties in the short sequence (*8*−*12*), we can ascribe differences in the ^{13}C chemical shift changes of M-Enk between PC binding and PS binding to different intermolecular binding interactions.

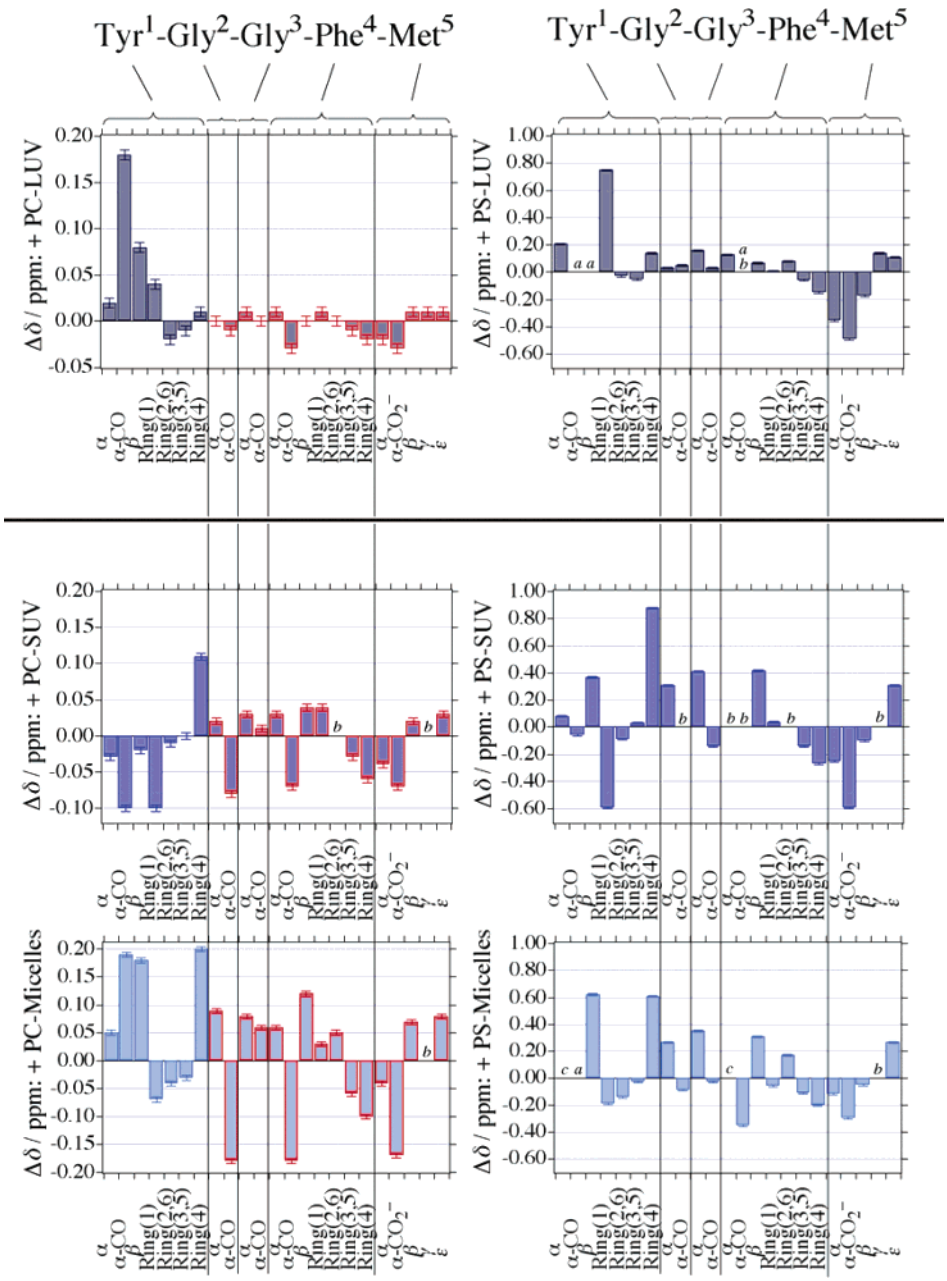

FIGURE 2: Observed ^{13}C chemical shift changes $\Delta\delta$ in M-Enk upon PC binding or PS binding in the LUV (top), SUV (middle), and micelles (bottom). Footnotes: *a*, value not determined because of line broadening; *b*, value not determined because of an overlap with the lipid signal; *c*, signals could not be unambiguously assigned.

Table 1 lists the ^{13}C chemical shift changes ($\Delta\delta$) of M-Enk induced by the binding to the PC−LUV or PS−LUV. Compare the $\Delta\delta$ values illustrated as bar graphs on the top panel of Figure 2. PS binding induces much a larger chemical shift change ($\Delta\delta$) than PC binding does at most of the peptide carbon sites; note the different axis scale. The larger $\Delta\delta$ values indicate highly preferred PS binding to PC binding as observed in the signal broadening. The following trends are notable in the PS binding: (1) marked upfield shifts ($\Delta\delta < 0$) in the C-terminal Met^5 at the α-C, β-C, and α-CO_2^- carbons and (2) downfield shifts ($\Delta\delta > 0$) in the N-terminal Tyr^1 at the ring-C(1) carbon. In contrast, in the PC binding marked shifts are only the downfield shifts ($\Delta\delta > 0$) in the N-terminal Tyr^1.

The upfield shifts $\Delta\delta$ in the PS binding are ascribed as follows to the electrostatic association (salt bridge) between the peptide C-terminal α-CO_2^- and the positively charged group in PS, i.e., headgroup NH_3^+. The observed relative magnitude of the upfield shifts $\Delta\delta$ in the C-terminus, α-CO_2^- (−0.49 ppm) > α-C (−0.35 ppm) > β-C (−0.17 ppm), is congruent with the relative magnitude reported on the protonation of the C-terminal CO_2^- in the pH titration, α-CO_2^- (−3.0 ppm) > α-C (−2.6 ppm) > β-C (−1.2 ppm) (*33*, *34*). The smaller shifts $\Delta\delta$ upon PS binding than the ones upon pH titration are because of the membrane-bound fraction of M-Enk at ∼15% compared to the full protonation (100%) in the titration. Thus it is considered that the electrostatic association between the C-terminal CO_2^- and the headgroup NH_3^+ is in contact to result in charge neutralization. When those neutralized amino and carboxyl groups separate thereafter with a less attractive potential, they are likely to regain charges solvated by water molecules that

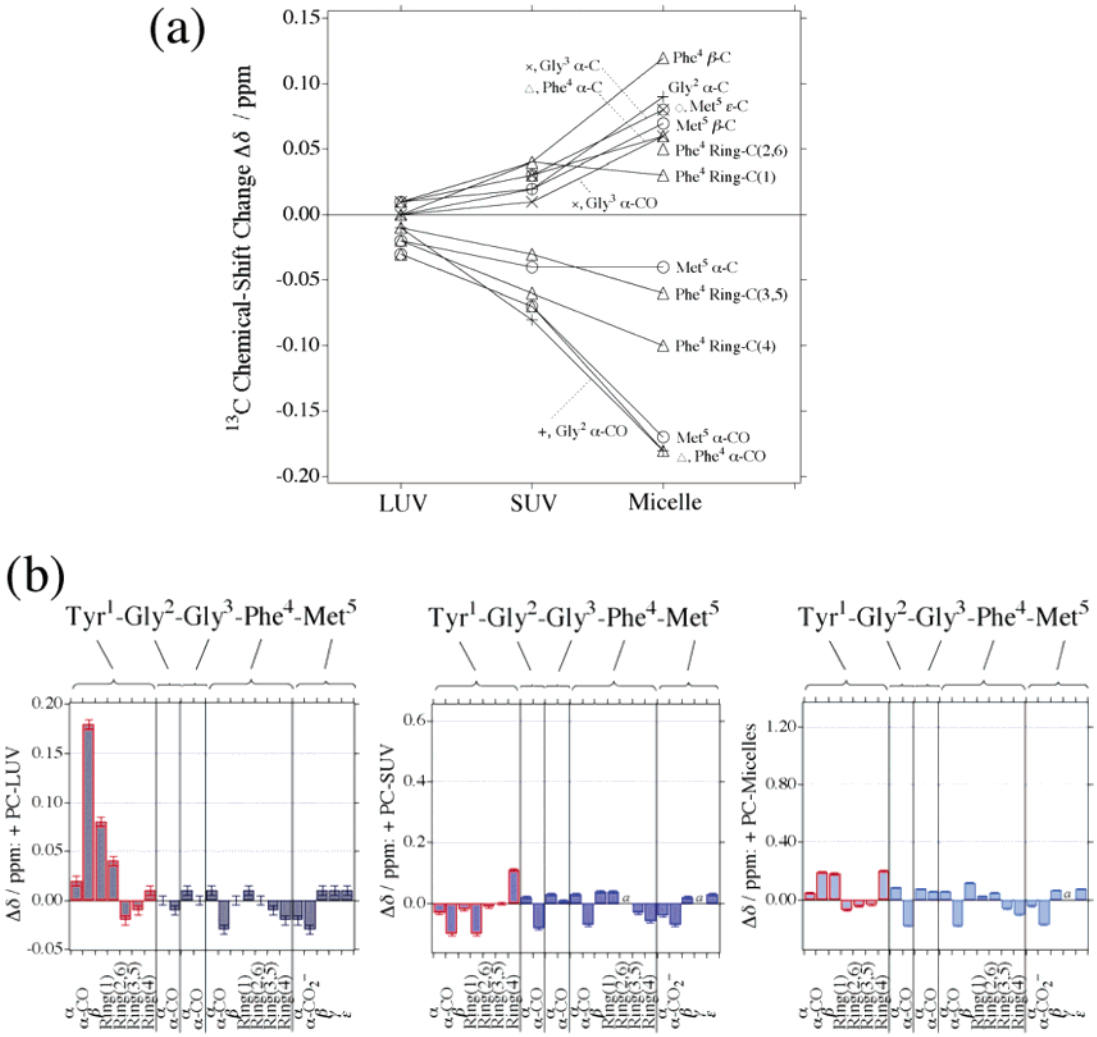

FIGURE 3: (a) Plots of ^{13}C chemical shift changes Δδ of M-Enk in residues other than the N-terminal Tyr^1, i.e., Gly^2-Gly^3-Phe^4-Met^5, upon PC binding in the LUV, SUV, and micelles. (b) ^{13}C chemical shift changes Δδ of M-Enk upon PC binding in the LUV, SUV, and micelles. Axis scales in the graphs for the SUV and micelle systems are expanded by a factor of 3.2 and 6.8, respectively, to adjust for comparison of the Δδ values in Gly^2-Gly^3-Phe^4-Met^5 to those for the LUV system. Footnote: *a*, value not determined because of an overlap with the lipid signal.

are abundant in the headgroup region of the membrane (*35*). The headgroup NH_3^+ locates below the headgroup CO_2^- and PO_4^- on the PS membrane surface (*18*), so that the magnitude of the upfield shifts Δδ in the C-terminus may in part be ascribed to accompanying dehydration; dehydration causes upfield changes in the ^{1}H and ^{13}C chemical shifts (*3*, *36*−*40*). Upon binding to the PC−LUV, in contrast, no prominent upfield shift Δδ in the C-terminus was observed. The absence of such shifts Δδ points out a shallow penetration of the C-terminal CO_2^- on the PC membrane surface without significant dehydration (*3*, *24*). The electrostatic binding site is most likely to be around the headgroup $N(CH_3)_3^+$ in PC which locates at the most superficial region of the membrane. Note that the electrostatic association of the C-terminal CO_2^- with the PC headgroup $N(CH_3)_3^+$ does not induce the characteristic upfield shifts as observed in the PS system because of the aprotic nature of the positive group. Thus, M-Enk anchors the C-terminus on the PS membrane surface, while it does not on the PC membrane surface.

As the zwitterionic counterpart of the C-terminal CO_2^- in M-Enk, the binding location of the N-terminal NH_3^+ on the surface of the PC and the PS membranes is examined. Prominent downfield shifts Δδ in the N-terminus are observed both upon PC binding and upon PS binding. The observation is ascribed to the electrostatic association with the headgroup negative charge(s) (PO_4^- in PC, CO_2^- and/or PO_4^- in PS); release of a proton in the NH_3^+ induces downfield shifts at carbons in the vicinity of the functional group (*33*, *34*, *41*, *42*). The Δδ values in the N-terminus upon PC binding exhibit the relative magnitude α-CO (+0.18 ppm) > β-C (+0.08 ppm) > α-C (+0.02 ppm), which is congruent with the relative magnitude reported on deprotonation of the N-terminal NH_3^+ in pH titration, α-CO (+6.9 ppm) > β-C (+3.1 ppm) > α-C (+1.0 ppm) (*33*, *34*). The smaller changes Δδ observed for the PC binding by a factor of a few percent are due to the membrane-bound fraction at a few percent. Upon PS binding, such quantitative information was not available because of the extreme signal broadening; however, the electrostatic association between the N-terminal NH_3^+ and the negative charge(s) in the anionic PS headgroup is very likely to take place, if it does in the zwitterionic PC as quantitatively disclosed above.

Binding Interactions in SUV and Micelles. Let us scrutinize finally how the site−site binding interactions revealed above

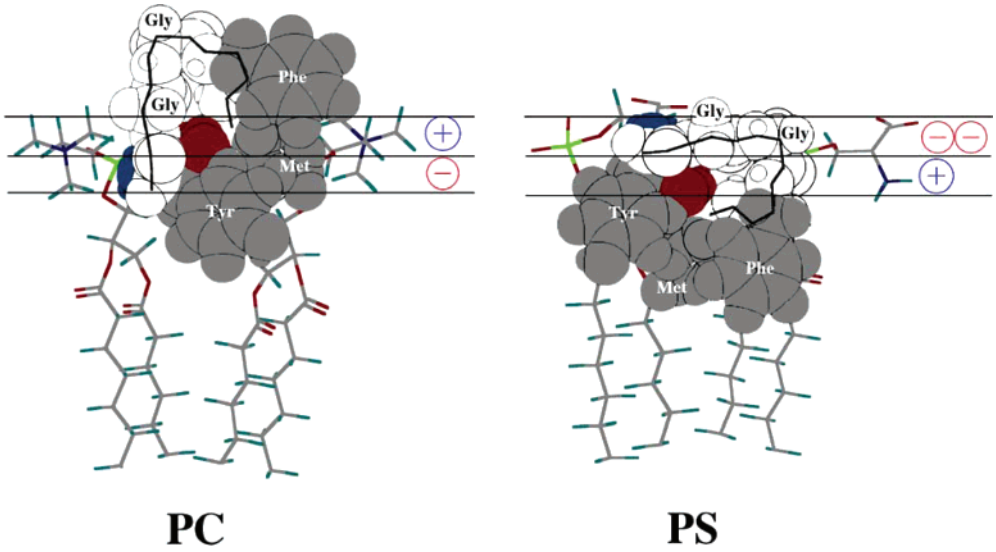

FIGURE 4: Models of M-Enk binding on the surfaces of the PC and the PS membranes according to the ^{13}C NMR data on peptide−lipid interactions. For lipids, the colors represent atomic elements as follows: light blue (H), gray (C), blue (N), red (O), and yellowish green (P). For M-Enk, the colors are used to denote the types of chemical groups: blue (NH_3^+), red (CO_2^-), white (backbone), and gray (hydrophobic side chains). A thick black line shows a track of the backbone for β-turn (*9*). On the headgroup structures of PC and PS in membranes (*17*), we can find contrastive charge alignments ($+1 \rightarrow -1 \rightarrow 0$) for PC and ($-2 \rightarrow +1 \rightarrow 0$) for PS from the surface to the hydrophobic core. The folded conformation in M-Enk (*9*) separates the cluster of hydrophobic Tyr^1, Phe^4, and Met^5 side chains from the hydrophilic N-terminal NH_3^+, C-terminal CO_2^-, and the two Gly residues.

by adopting the LUV membrane are sensitive or not to the membrane-surface curvature. A curvature increase may alter the binding interactions significantly through the enhanced degrees of hydration and of structural fluctuations of the membrane lipids. The diameter of the lipid particles is varied from the LUV (∼100 nm) to the micelles (∼5 nm).

Prominent downfield shifts $\Delta\delta$ (>0) of the ^{13}C signals in the N-terminal Tyr^1 were observed upon binding to the PC−LUV, whereas as shown in Figure 2 no such prominent shift $\Delta\delta$ was observed upon binding to the PC−SUV or −micelles. Binding to the PC, forming SUV or micelles, induces the shifts $\Delta\delta$ in the N-terminal Tyr^1 only in comparable magnitude with the shifts $\Delta\delta$ in the other residues. Such a drastic difference in the binding effect on M-Enk chemical shift values between the LUV and the smaller lipid particles is obvious for the PS binding as well. Prominence of the downfield shifts $\Delta\delta$ in the N-terminal Tyr^1 and of the upfield shifts in the C-terminal Met^5 observed upon binding to PS in the LUV is absent for PS in the SUV or micelles. The lost prominence of the shifts $\Delta\delta$ in the N- and C-terminal residues tells that the role of peptide−lipid electrostatic associations becomes less notable in stabilizing the binding state compared to the roles played in the other part of the peptide structure. This is probably due to the presence of stronger hydration and larger structural fluctuations because of the highly curved membrane surface.

We note that in the PC systems the carbon site dependence of $\Delta\delta$ in residues other than the N-terminal Tyr^1, i.e., Gly^2-Gly^3-Phe^4-Met^5, is highly conserved for the membranes with the different surface curvature; the $\Delta\delta$ values in those residues increase in parallel with increasing surface curvature (see Figure 3a). How then can the carbon site dependence of $\Delta\delta$ be conserved upon drastic changes in the degrees of hydration and motional fluctuations of lipids with increasing curvature? As presented above on the electrostatic interactions between the peptide termini and the lipid headgroups, the curvature increase alters the intermolecular peptide−lipid interactions in a nonsystematic manner. It can thus be deduced that the conserved carbon site dependence of $\Delta\delta$ in the residues Gly^2-Gly^3-Phe^4-Met^5 stems from the conserved intramolecular (conformational) effect on the chemical shifts upon binding. The absence of perturbation on the chemical shifts in those residues except by the conformational effect indicates exposure of this structural moiety Gly^2-Gly^3-Phe^4-Met^5 from the binding interface with the PC membrane. Actually, the membrane-bound enkephalin is known to take a compact folded conformation independent of the membrane type, such as micelles, bicelles, and vesicles as referred to above. If we adjust for comparison the magnitude scale for the $\Delta\delta$ values in residues Gly^2-Gly^3-Phe^4-Met^5 due to the conformational effect (Figure 3b), it is confirmed that the intermolecular binding interactions at the N-terminal Tyr^1 are drastically dependent on the membrane type. The conclusion of the exposure of the residues other than the N-terminal Tyr^1 on the PC membrane surface is in agreement with a UV resonance Raman study adopting the SUV, which provided information on the locations of the two aromatic rings; the Tyr^1 ring is inserted into the membrane, while the Phe^4 ring is either exposed to the aqueous phase or in the polar headgroup region (*11*). Similar observations of the different binding depth between the Tyr^1 and Phe^4 rings have been reported recently in the case of leucine-enkephalin as well (*13*). Here the ^{13}C NMR results show that M-Enk shallowly binds to the PC−membrane surface only by inserting the N-terminal Tyr^1; i.e., the other residues are exposed to the environment abundant in water molecules.

CONCLUSIONS

By means of natural-abundance ^{13}C NMR spectroscopy, enkephalin−phospholipid binding interactions on the surface of zwitterionic PC and anionic PS membranes are studied. Binding interactions could be sensitively monitored when a membrane system with negligible surface curvature like the LUV was adopted. The binding state of the folded M-Enk

on the surfaces of the PC and the PS membranes can be modeled as in Figure 4 according to the NMR information.

On the PS membrane surface, the charged (both positive and negative) and uncharged groups in M-Enk and PS fit in one another to allow efficient electrostatic and hydrophobic interactions; the peptide N-terminal NH_3^+ is attracted by the PS headgroup CO_2^- and/or PO_4^-, the C-terminal CO_2^- is attracted by the headgroup NH_3^+, and the hydrophobic side chains are anchored to the uncharged region below the ionic headgroups. The charge cancellation between M-Enk and lipids stabilizes the binding state by compensating for the electrostatic hydration free energy of the ionic groups in the free peptide (*3*, *24*, *25*) and lipid headgroups (*26*−*28*). The anchoring of hydrophobic side chains cooperatively assists the strong binding. Such a hydrophobic effect is subordinate in the present case of enkephalin binding according to the location of the hydrophobic side chains around the polar groups just below the strongly associating peptide terminal and lipid headgroup ions.

On the PC membrane surface, the effective peptide−lipid binding interactions are obviously less than those on the PS membrane surface. The N-terminal NH_3^+ is attracted by the headgroup PO_4^-, and the hydrophobic Tyr^1 in the N-terminus is inserted to the uncharged region. The other residues Gly^2-Gly^3-Phe^4-Met^5 are exposed from the binding interface with the membrane. If we force the hydrophobic side chains to be anchored as in the PS membrane with the N-terminal NH_3^+ bound at the negatively charged PO_4^- and the Tyr^1 residue bound in the uncharged region, it is obvious that the binding state becomes less stabilized; the destabilizing effect arises from the burial of the strongly hydrated C-terminal CO_2^- into the uncharged region even under the repulsive negative layer due to the PO_4^-.

As a result of the effective peptide−lipid binding interactions due to the harmonious distributions of charged and uncharged groups along the bilayer normal, M-Enk binds deeper and stronger on the PS membrane surface than on the PC membrane surface. The importance of such electrostatic site−site binding interactions is emphasized as a controlling factor of the binding location and orientation of M-Enk; note the smaller lateral area per lipid molecule in the PS than in the PC membranes (*43*). In diverse lipid environments in nerve cells, a similar role played by the local charge distributions on the membrane surface along the bilayer normal is proposed to be significant in regulating the binding of neuropeptides, besides roles of the charge distributions in the surface plane particularly where microdomains like rafts (*44*) are present.

ACKNOWLEDGMENT

The author is grateful to Professor Emeritus Yukio Sugiura of Kyoto University on use of the 600 MHz NMR spectrometer, to Professor Masaru Nakahara for providing materials as well as helpful discussions, and to Professors Aoyama and Oka on use of the ultracentrifugation apparatus. The author thanks Dr. Tsuguhiro Kimura of Kyoto University for guidance of profound medical background of the nervous functions.

SUPPORTING INFORMATION AVAILABLE

^1H NMR spectra showing drastic slowdown in dynamics of the molecular environment around M-Enk upon binding to PS large unilamellar vesicles. This material is available free of charge via the Internet at http://pubs.acs.org.

NOTE ADDED AFTER ASAP PUBLICATION

This paper was published ASAP 12/01/06. There was a production error in the last paragraph of the Results and Discussion section. The corrected version was published ASAP 12/07/06.

REFERENCES

1. Simon, S. A., and McIntosh, T. J., Eds. (2002) *Peptide-Lipid Interactions*, Academic Press, San Diego, CA.
2. Epand, R. M., Ed. (1997) *Lipid Polymorphism and Membrane Properties*, Academic Press, San Diego, CA.
3. Kimura, T., Okamura, E., Matubayasi, N., Asami, K., and Nakahara, M. (2004) NMR study on the binding of neuropeptide achatin-I to phospholipid bilayer: The equilibrium, location, and peptide conformation, *Biophys. J. 87*, 375−385.
4. Sargent, D. F., and Schwyzer, R. (1986) Membrane lipid phase as catalyst for peptide-receptor interactions, *Proc. Natl. Acad. Sci. U.S.A. 83*, 5774−5778.
5. Gysin, B., and Schwyzer, R. (1983) Head group and structure specific interactions of enkephalins and dynorphin with liposomes: investigation by hydrophobic photolabeling, *Arch. Biochem. Biophys. 225*, 467−474.
6. Hughes, J., Smith, T. W., Kosterlitz, H. W., Fothergill, L. A., Morgan, B. A., and Morris, H. R. (1975) Identification of two related pentapeptides from the brain with potent opiate agonist activity, *Nature 258*, 577−579.
7. Jarrell, H. C., Deslauriers, R., McGregor, W. H., and Smith, I. C. P. (1980) Interaction of opioid peptides with model membranes. A carbon-13 nuclear magnetic study of enkephalin binding to phosphatidylserine, *Biochemistry 19*, 385−390.
8. Milon, A., Miyazawa, T., and Higashijima, T. (1990) Transferred nuclear Overhauser effect analyses of membrane-bound enkephalin analogues by ^1H nuclear magnetic resonance: Correlation between activities and membrane-bound conformations, *Biochemistry 29*, 65−75.
9. Behnam, B. A., and Deber, C. M. (1984) Evidence for a folded conformation of methionine- and leucine-enkephalin in a membrane environment, *J. Biol. Chem. 259*, 14935−14940.
10. Surewicz, W. K., and Mantsch, H. H. (1988) Solution and membrane structure of enkephalins as studied by infrared spectroscopy, *Biochem. Biophys. Res. Commun. 150*, 245−251.
11. Takeuchi, H., Ohtsuka, Y., and Harada, I. (1992) Ultraviolet resonance Raman study on the binding mode of enkephalin to phospholipid membranes, *J. Am. Chem. Soc. 114*, 5321−5328.
12. Marcotte, I., Separovic, F., Auger, M., and Gagné, S. M. (2004) A multidimensional ^1H NMR investigation of the conformation of methionine-enkephalin in fast-tumbling bicelles, *Biophys. J. 86*, 1587−1600.
13. Chandrasekhar, I., van Gunsteren, W. F., Zandomeneghi, G., Williamson, P. T. F., and Meier, B. H. (2006) Orientation and conformational preference of leucine-enkephalin at the surface of a hydrated dimyristoylphosphatidylcholine bilayer: NMR and MD simulation, *J. Am. Chem. Soc. 128*, 159−170.
14. Tancrède, P., Deslauriers, R., McGregor, W. H., Ralston, E., Sarantakis, D., Somorjai, R. L., and Smith, I. C. P. (1978) A carbon-13 nuclear magnetic resonance study of the molecular dynamics of methionine-enkephalin and α-endorphin in aqueous solution, *Biochemistry 17*, 2905−2914.
15. Deber, C. M., and Behnam, B. A. (1984) Role of membrane lipids in peptide hormone function: Binding of enkephalins to micelles, *Proc. Natl. Acad. Sci. U.S.A. 81*, 61−65.
16. Marcotte, I., Dufourc, E. J., Ouellet, M., and Auger, M. (2003) Investigation of the neuropeptide Met-enkephalin with zwitterionic and negatively charged bicelles as viewed by ^{31}P and ^2H solid-state NMR, *Biophys. J. 85*, 328−339.
17. Marcotte, I., Ouellet, M., and Auger, M. (2004) Insights on the interaction of Met-enkephalin with negatively charged membranes: An infrared and solid-state NMR spectroscopic study, *Chem. Phys. Lipids 127*, 175−187.
18. Pandit, S. A., Bostick, D., and Berkowitz, M. L. (2003) Mixed bilayer containing dipalmitoylphosphatidylcholine and dipalmi-

toylphosphatidylserine: Lipid complexation, ion binding, and electrostatics,*Biophys. J. 85*, 3120−3131.
19. Higashijima, T., Kobayashi, J., Nagai, U., and Miyazawa, T. (1979) Nuclear-magnetic-resonance study on Met-enkephalin and Met-enkephalinamide, *Eur. J. Biochem. 97*, 43−57.
20. Kinoshita, M., Okamoto, Y., and Hirata, F. (1997) Solvation structure and stability of peptides in aqueous solutions analyzed by the reference interaction site model theory, *J. Chem. Phys. 107*, 1586−1599.
21. Koynova, R., and Caffrey, M. (1998) Phases and phase transitions of the phosphatidylcholines, *Biochim. Biophys. Acta 1376*, 91−145.
22. Sheetz, M. P., and Chan, S. I. (1972) Effect of sonication on the structure of lecithin bilayers, *Biochemistry 11*, 4573−4581.
23. Markley, J. L., and Opella, S. J., Eds. (1997) *Biological NMR Spectroscopy*, Oxford University, New York, NY.
24. Kimura, T., Matubayasi, N., and Nakahara, M. (2004) Side-chain conformational thermodynamics of aspartic acid residue in the peptides and achatin-I in aqueous solution, *Biophys. J. 86*, 1124−1137.
25. Kimura, T., Matubayasi, N., Sato, H., Hirata, F., and Nakahara, M. (2002) Enthalpy and entropy decomposition of free-energy changes for side-chain conformations of aspartic acid and asparagine in acidic, neutral, and basic aqueous solutions, *J. Phys. Chem. B 106*, 12336−12343.
26. Simon, S. A., and McIntosh, T. J. (1989) Magnitude of the solvation pressure depends on dipole potential, *Proc. Natl. Acad. Sci. U.S.A. 86*, 9263−9267.
27. Gawrisch, K., Ruston, D., Zimmerberg, J., Parsegian, V. A., Rand, R. P., and Fuller, N. (1992) Membrane dipole potentials, hydration forces, and the ordering of water at membrane surfaces, *Biophys. J. 61*, 1213−1223.
28. Saiz, L., and Klein, M. L. (2002) Electrostatic interactions in a neutral model phospholipid bilayer by molecular dynamics simulations, *J. Chem. Phys. 116*, 3052−3057.
29. Szoka, F., Jr., and Papahadjopoulos, D. (1980) Comparative properties and methods of preparation of lipid vesicles (liposomes), *Annu. Rev. Biophys. Bioeng. 9*, 467−508.
30. Mattai, J., Hauser, H., Demel, R. A., and Shipley, G. G. (1989) Interactions of metal ions with phosphatidylserine bilayer membranes: Effect of hydrocarbon chain unsaturation, *Biochemistry 28*, 2322−2330.
31. Okamura, E., Wakai, C., Matubayasi, N., and Nakahara, M. (1997) ^{14}N NMR spectra sensitively reflect surface curvature and segmental motion of hydrophilic headgroups in lipid bilayers and micelles, *Chem. Lett.*, 1061−1062.
32. Khaled, M. A., Urry, D. W., and Bradley, R. J. (1979) pH and solvent titration of enkephalins by carbon-13 nuclear magnetic resonance spectroscopy: Complete assignments of resonances, *J. Chem. Soc., Perkin Trans. 2*, 1693−1699.
33. Wüthrich, K. (1976) *NMR in Biological Research: Peptides and Proteins*, North-Holland Publishing Co., Amsterdam, The Netherlands.
34. Christl, M., and Roberts, J. D. (1972) Nuclear magnetic resonance spectroscopy. Carbon-13 chemical shifts of small peptides as a function of pH, *J. Am. Chem. Soc. 94*, 4565−4573.
35. Wiener, M. C., and White, S. H. (1992) Structure of a fluid dioleoylphosphatidylcholine bilayer determined by joint refinement of x-ray and neutron diffraction data: III. Complete structure, *Biophys. J. 61*, 434−447.
36. Buckingham, A. D., Schaefer, T., and Schneider, W. G. (1960) Solvent effects in nuclear magnetic resonance spectra, *J. Chem. Phys. 32*, 1227−1233.
37. Becker, E. D. (1980) *High Resolution NMR: Theory and Chemical Applications*, 2nd ed., Academic Press, New York, NY.
38. Rao, U. R. K., Manohar, C., Valaulikar, B. S., and Iyer, R. M. (1987) Micellar chain model for the origin of the viscoelasticity in dilute surfactant solutions, *J. Phys. Chem. 91*, 3286−3291.
39. Okamura, E., and Nakahara, M. (1999) NMR study directly determining drug delivery sites in phospholipid bilayer membranes, *J. Phys. Chem. B 103*, 3505−3509.
40. Jackowski, K., Wilczek, M., Pecul, M., and Sadlej, J. (2000) Nuclear magnetic shielding and spin-spin coupling of 1,2-^{13}C-enriched acetylene in gaseous mixtures with xenon and carbon dioxide, *J. Phys. Chem. A 104*, 5955−5958.
41. Quirt, A. R., Lyerla, J. R., Jr., Peat, I. R., Cohen, J. S., Reynolds, W. F., and Freedman, M. H. (1974) Carbon-13 nuclear magnetic resonance titration shifts in amino acids, *J. Am. Chem. Soc. 96*, 570−574.
42. Slichter, C. P. (1990) *Principles of Magnetic Resonance*, 3rd enlarged and updated ed., Springer-Verlag, Berlin, Germany.
43. Petrache, H. I., Tristram-Nagle, S., Gawrisch, K., Harries, D., Parsegian, V. A., and Nagle, J. F. (2004) Structure and fluctuations of charged phosphatidylserine bilayers in the absence of salt, *Biophys. J. 86*, 1574−1586.
44. Epand, R. F., Sayer, B. G., and Epand, R. M. (2005) Induction of raft-like domains by a myristoylated NAP-22 peptide and its Tyr mutant, *FEBS J. 272*, 1792−1803.

BI061641V